DiDonato J, Mercurio F, Rosette C, Wu-Li J, Suyang H, Ghosh S, and Karin M (1996) Mapping of the inducible IkappaB phosphorylation sites that signal its ubiquitination and degradation. *Mol Cell Biol* **16**:1295–1304.

Dignam JD, Lebovitz RM, and Roeder RG (1983) Accurate transcription initiation by RNA polymerase II in a soluble extract from isolated mammalian nuclei. *Nucleic Acids Res* **11**:1475–1489.

Fujiwara H, Arima N, Otsubo H, Matsushita K, Hidaka S, Arimura K, Kukita T, Yamaguchi K, and Tanaka H (1997) Vesnarinone exhibits antitumor effect against myeloid leukemia cells via apoptosis. *Exp Hematol* **25**:1180–1186.

Hellerbrand C, Jobin C, Iimuro Y, Licato L, Sartor RB, and Brenner DA (1998) Inhibition of NFkappaB in activated rat hepatic stellate cells by proteasome inhibitors and an IkappaB super-repressor. *Hepatology* **27**:1285–1295.

Hiramoto M, Kawakami Y, Nabeshima R, Shima D, Handa H, and Aizawa S (2004) Identification of differentiation-inducing activity produced by human bone marrow stromal cell line LP101. *Int J Mol Med* **14**:867–872.

Honma Y, Yamamoto-Yamaguchi Y, and Kanatani Y (1999) Vesnarinone and glucocorticoids cooperatively induce G1 arrest and have an anti-tumour effect on human non-small cell lung carcinoma cells grown in nude mice. *Br J Cancer* **80**:96–103.

Ito T, Ando H, Suzuki T, Ogura T, Hotta K, Imamura Y, Yamaguchi Y, and Handa H (2010) Identification of a primary target of thalidomide teratogenicity. *Science* **327**:1345–1350.

Itoh H, Kusagawa M, Shimomura A, Suga T, Ito M, Konishi T, and Nakano T (1993) Ca2+(-)dependent and Ca2+(-)independent vasorelaxation induced by cardiotonic phosphodiesterase inhibitors. *Eur J Pharmacol* **240**:57–66.

Ju J-S, Fuentealba RA, Miller SE, Jackson E, Piwnica-Worms D, Baloh RH, and Weihl CC (2009) Valosin-containing protein (VCP) is required for autophagy and is disrupted in VCP disease. *J Cell Biol* **187**:875–888.

Kubo K, Matsuzaki Y, Kato A, Terai S, and Okita K (1999) Antitumor effect of vesnarinone on human hepatocellular carcinoma cell lines. *Int J Oncol* **14**:41–46.

Manna SK and Aggarwal BB (2000) Vesnarinone suppresses TNF-induced activation of NF-kappa B, c-Jun kinase, and apoptosis. *J Immunol* **164**:5815–5825.

Matsui S, Matsumori A, Matoba Y, Uchida A, and Sasayama S (1994) Treatment of virus-induced myocardial injury with a novel immunomodulating agent, vesnarinone. Suppression of natural killer cell activity and tumor necrosis factor-alpha production. *J Clin Invest* **94**:1212–1217.

Meerang M, Ritz D, Paliwal S, Garajova Z, Bosshard M, Mailand N, Janscak P, Hübscher U, Meyer H, and Ramadan K (2011) The ubiquitin-selective segregase VCP/p97 orchestrates the response to DNA double-strand breaks. *Nat Cell Biol* **13**:1376–1382.

Meyer H, Bug M, and Bremer S (2012) Emerging functions of the VCP/p97 AAA-ATPase in the ubiquitin system. *Nat Cell Biol* **14**:117–123.

Nabeshima R, Aizawa S, Nakano M, Toyama K, Sugimoto K, Kaidow A, Imai T, and Handa H (1997) Effects of vesnarinone on the bone marrow stromal cell-dependent proliferation and differentiation of HL60 cells in vitro. *Exp Hematol* **25**:509–515.

Nio Y, Ohmori H, Minari Y, Hirahara N, Sasaki S, Takamura M, and Tamura K (1997) A quinolinone derivative, vesnarinone (OPC-8212), significantly inhibits the in vitro and in vivo growth of human pancreatic cancer cell lines. *Anticancer Drugs* **8**:686–695.

Nishio K, Masaike Y, Ikeda M, Narimatsu H, Gokon N, Tsubouchi S, Hatakeyama M, Sakamoto S, Hanyu N, Sandhu A et al. (2008) Development of novel magnetic nano-carriers for high-performance affinity purification. *Colloids Surf B Biointerfaces* **64**:162–169.

Nishizawa M, Fu S-L, Kataoka K, and Vogt PK (2003) Artificial oncoproteins: modified versions of the yeast bZip protein GCN4 induce cellular transformation. *Oncogene* **22**:7931–7941.

Ogino S, Tsuruma K, Uehara T, and Nomura Y (2004) Herbimycin A abrogates nuclear factor-kappaB activation by interacting preferentially with the IkappaB kinase beta subunit. *Mol Pharmacol* **65**:1344–1351.

Ritz D, Vuk M, Kirchner P, Bug M, Schütz S, Hayer A, Bremer S, Lusk C, Baloh RH, Lee H et al. (2011) Endolysosomal sorting of ubiquitylated caveolin-1 is regulated by VCP and UBXD1 and impaired by VCP disease mutations. *Nat Cell Biol* **13**:1116–1123.

Roff M, Thompson J, Rodriguez MS, Jacque JM, Baleux F, Arenzana-Seisdedos F, and Hay RT (1996) Role of IkappaBalpha ubiquitination in signal-induced activation of NFkappaB in vivo. *J Biol Chem* **271**:7844–7850.

Sato Y, Matsumori A, and Sasayama S (1995) Inotropic agent vesnarinone inhibits cytokine production and E-selectin expression in human umbilical vein endothelial cells. *J Mol Cell Cardiol* **27**:2265–2273.

Shimizu N, Sugimoto K, Tang J, Nishi T, Sato I, Hiramoto M, Aizawa S, Hatakeyama M, Ohba R, Hatori H et al. (2000) High-performance affinity beads for identifying drug receptors. *Nat Biotechnol* **18**:877–881.

Sunwoo JB, Chen Z, Dong G, Yeh N, Crowl Bancroft C, Sausville E, Adams J, Elliott P, and Van Waes C (2001) Novel proteasome inhibitor PS-341 inhibits activation of nuclear factor-kappa B, cell survival, tumor growth, and angiogenesis in squamous cell carcinoma. *Clin Cancer Res* **7**:1419–1428.

Yatani A, Imoto Y, Schwartz A, and Brown AM (1989) New positive inotropic agent OPC-8212 modulates single Ca^{2+} channels in ventricular myocytes of guinea pig. *J Cardiovasc Pharmacol* **13**:812–819.

Yen CH, Yang YC, Ruscetti SK, Kirken RA, Dai RM, and Li CC (2000) Involvement of the ubiquitin-proteasome pathway in the degradation of nontyrosine kinase-type cytokine receptors of IL-9, IL-2, and erythropoietin. *J Immunol* **165**:6372–6380.

Yokozaki H, Ito R, Ono S, Hayashi K, and Tahara E (1999) Effect of 3,4-dihydro-6-[4-(3,4-dimethoxybenzoyl)-1-piperazinyl]-2(1H)- quinolinone (vesnarinone) on the growth of gastric cancer cell lines. *Cancer Lett* **140**:121–128.

Address correspondence to: Dr. Hiroshi Handa, Graduate School of Bioscience and Biotechnology, Tokyo Institute of Technology, 4259 Nagatsuda-cho, Midori-ku, Yokohama, 226-8503, Japan. E-mail: handa.h.aa@m.titech.ac.jp

Induction of Rapid T Cell Death and Phagocytic Activity by Fas-Deficient *lpr* Macrophages

Ritsuko Oura,*,† Rieko Arakaki,* Akiko Yamada,* Yasusei Kudo,* Eiji Tanaka,† Yoshio Hayashi,* and Naozumi Ishimaru*

Peripheral T cells are maintained by the apoptosis of activated T cells through the Fas–Fas ligand system. Although it is well known that normal T cells fail to survive in the Fas-deficient immune condition, the molecular mechanism for the phenomenon has yet to be elucidated. In this study, we demonstrate that rapid cell death and clearance of normal T cells were induced by Fas-deficient *lpr* macrophages. Transfer of normal T cells into *lpr* mice revealed that Fas expression on donor T cells was promptly enhanced through the IFN-γ/IFN-γR. In addition, Fas ligand expression and phagocytic activity of *lpr* macrophages were promoted through increased NF-κB activation. Controlling Fas expression on macrophages plays an essential role in maintaining T cell homeostasis in the peripheral immune system. Our data suggest a critical implication to the therapeutic strategies such as transplantation and immunotherapy for immune disorder or autoimmunity related to abnormal Fas expression. *The Journal of Immunology*, **2013, 190: 578–585.**

The Fas receptor is expressed on most tissues and plays an important role in regulating the normal function of many different organs. Fas signaling can regulate T cell and B cell differentiation, maturation, activation, and deletion in the peripheral immune system (1–3). Activation-induced cell death (AICD) is involved in the removal of activated T cells in vivo and depends on Fas and Fas ligand (FasL) (4, 5). Among apoptotic mechanisms, AICD plays a central role in the removal of autoreactive T cells and in prevention of autoimmune responses (6).

MRL/Mp mice bearing a Fas deletion mutant gene, *lpr* (MRL/*lpr*), spontaneously develop autoimmune lesions resembling human glomerulonephritis, arthritis, vasculitis, and Sjögren's syndrome (7–10). In addition, *gld* mice defective in the FasL gene exhibit autoimmune lesions (11). Both strains lack the cell death mechanism mediated through the Fas–FasL interaction in the immune system. Ligation of Fas by the homotrimeric FasL results in the clustering of Fas and recruitment of the adaptor protein Fas-associated death domain to clustered Fas intracellular death domains (5, 12–14). In addition, Fas and only the Bcl2 homology domain 3 (BH3-only protein) such as Bim play overlapping roles in peripheral T cell death in immune response shutdown and prevention of immune disorders (15). In contrast, the regulation of T cell susceptibility to AICD is controlled by T cell maturity and activation and the presence or absence of APCs such as macrophages or dendritic cells (5, 16).

Normal hematopoietic cells including spleen and bone marrow cells do not survive in *lpr* mice (17, 18). In addition, it was reported that in vitro coculture of normal and *lpr*-derived T cell lines resulted in the loss of the normal T cells (17, 19). These in vivo and in vitro findings could be explained by the elevated FasL expression on *lpr* immune cells (20, 21). However, the precise mechanism underlying the FasL overexpression in *lpr* immune cells or the association of normal T cell deletion with APCs in Fas-deficient *lpr* mice remains unclear.

In this study, we focused on T cell apoptosis in Fas-deficient recipients using C57BL/6/*lpr* mice to define the cellular and molecular mechanisms of AICD in T cells and the regulation of FasL expression. Furthermore, we investigated whether macrophages in Fas-deficient *lpr* mice contribute to the clearance of apoptotic T cells in the peripheral immune system.

Materials and Methods

Mice

C57BL/6 (B6), B6-*lpr/lpr* (B6/*lpr*), and B6-*gld/gld* (B6/*gld*) mice were purchased from Japan SLC Laboratory (Shizuoka, Japan). OT-II mice (C57BL/6-Tg (TcraTcrb) 425Cbn/J) and IFN-γR gene knockout (*IFNγR*$^{-/-}$) mice were obtained from Dr. J. Sprent. *NF-κB*$_1$$^{-/-}$ mice were obtained from The Jackson Laboratory. GFP-transgenic (TG) mice were obtained from RIKEN BioResource Center (Tsukuba, Japan). All mice were bred at the animal facility of the University of Tokushima under specific pathogen-free conditions. The experiments were approved by an animal ethics board of the University of Tokushima.

Adoptive cell transfer

T cells were purified from the spleen of B6, GFP-TG, OT-II, B6/*lpr*, or *IFNγR*$^{-/-}$ mice using Abs including anti-MHC class II, anti-B220 (eBioscience, San Diego, CA), and immunomagnetic beads (Dynal, Oslo, Norway). T cells from all mice, except GFP-TG mice, were labeled with CFSE (Invitrogen, Carlsbad, CA). A total of 1, 2, or 5×10^6 T cells were i.v. or i.p. transferred into B6, B6/*lpr*, B6/*gld*, or *NF-κB*$_1$$^{-/-}$/*lpr* mice. For homeostatic expansion, the recipient mice were irradiated at 8.5

*Department of Oral Molecular Pathology, Institute of Health Biosciences, University of Tokushima Graduate School, Tokushima 770-8504, Japan; and †Department of Orthodontics and Dentofacial Orthopedics, Institute of Health Biosciences, University of Tokushima Graduate School, Tokushima 770-8504, Japan

Received for publication December 28, 2011. Accepted for publication November 12, 2012.

This work was supported by the Funding Program for Next Generation World-Leading Researchers in Japan (Grant LS090) and by Grants-in-Aid for Scientific Research (17109016 and 17689049) from the Ministry of Education, Science, Sport and Culture of Japan.

Address correspondence and reprint requests to Dr. Naozumi Ishimaru, Department of Oral Molecular Pathology, Institute of Health Biosciences, University of Tokushima Graduate School, 3-18-15 Kuramotocho, Tokushima 770-8504, Japan. E-mail address: ishimaru@dent.tokushima-u.ac.jp

The online version of this article contains supplemental material.

Abbreviations used in this article: AICD, activation-induced cell death; B6, C57BL/6; B6/*gld*, C57BL/6-*gld/gld*; B6/*lpr*, C57BL/6-*lpr/lpr*; FasL, Fas ligand; *IFNγR*$^{-/-}$, IFN-γR gene knockout; LN, lymph node; PEC, peritoneal exudate cell; TG, transgenic.

www.jimmunol.org/cgi/doi/10.4049/jimmunol.1103794

Gy before T cell transfer. For the analysis of donor T cells, spleen cells, lymph node (LN) cells, PBMCs, or peritoneal exudate cells (PECs) were analyzed by flow cytometry. To inhibit in vivo deletion of T cells, anti-FasL mAb (clone MFL3; BioLegend, San Diego, CA) was i.p. injected into recipient mice together with transfer of T cells.

Flow cytometry

FITC, PE, allophycocyanin–peridin chlorophyll protein, PE-Cy5.5, PE-Cy7, or allophycocyanin–Cy7-conjugated Abs including anti-CD4, CD8, CD11b, Fas, and FasL Abs, were used. A FACScan flow cytometer (BD Biosciences, Franklin Lakes, NJ) was used, and data were analyzed using the FlowJo FACS Analysis software (Tree Star, Ashland, OR).

In vivo imaging

The mice were s.c. injected with isoflurane (Abbott Laboratories, Abbot Park, IL) as an anesthetic. Purified T cells were incubated with XenoLight DiR (Caliper Life Sciences, Hopkinton, MA) for 30 min. A total of 5×10^6 T cells were i.v. transferred into recipient mice, and donor T cells were monitored at 30 min, 2 h, and 6 h using in vivo imaging analyzer (Caliper Life Sciences).

ELISA

The concentration of IFN-γ in sera was measured by ELISA. Ninety-six-well flat-bottom plates were precoated with capture Abs, and diluted samples or standard recombinant cytokines were added to each well. After the plates were washed, biotinylated Abs were added, and the wells were incubated with HRP-labeled, affinity-purified anti-rat IgG. A solution of *o*-phenylenediamine (Sigma-Aldrich, St. Louis, MO) was added to each well as the substrate. The optimal density at 490 nm was measured using a microplate reader (Model 680; Bio-Rad Laboratories, Richmond, CA).

Quantitative RT-PCR

Total RNA was extracted from spleen cells or PECs using Isogen (Wako Pure Chemical Industries, Osaka, Japan); it was then reverse transcribed. The transcript levels of FasL, TNF-α, IL-6, IL-1β, and β-actin were performed using a PTC-200 DNA Engine Cycler (Bio-Rad Laboratories) with SYBR Premix Ex Taq (Takara Bio, Shiga, Japan). The primer sequences used were as follows: FasL, forward, 5′-GTGGGCCGCTCTAGGCACCA-3′, and reverse, 5′-CGGTTGGCCTTAGGGTTCAGGGGG-3′; TNF-α, forward, 5′-ATGAGCACAGAAAGCATGATC-3′, and reverse, 5′-AGATGATCTGAGTGTGAGGG-3′; IL-6, forward, 5′-CTCTGCAAGAGACTTCCAT-3′, and reverse, 5′-ATAGGCAAATTTCCTGATTATA-3′; IL-1β, forward, 5′-TGATGAGAATGACCTGTTCT-3′, and reverse, 5′-CTTCTTCAAAGATGAAGGAAA-3′; β-actin, forward, 5′-GTGGGCCGCTCTAGGCACCA-3′, and reverse, 5′-CGGTTGGCCTTAGGGTTCAGGGGG-3′.

Preparation of peritoneal macrophages

Mice were i.p. injected with 1 ml 3% thioglycollate broth (Sigma-Aldrich), and after 3 or 4 d, elicited macrophages were collected by peritoneal lavage with 5 ml ice-cold PBS.

Phagocytosis assay

Phagocytosis was assessed using Fluoresbrite Yellow Green Caboxylate Microspheres (Polysciences, Warrington, PA). Briefly, the $CD11b^+$ cells purified from PECs were incubated with opsonized beads for 30 min at 37°C and washed with PBS. The phagocytic activity of $CD11b^+$ cells was evaluated by flow cytometric analysis.

Apoptosis detection assay

Apoptosis was detected using the Annexin V-FITC apoptosis detection kit (Bio Vision, Mountain View, CA). Briefly, the cells were washed with PBS and incubated with FITC-conjugated annexin V and propidium iodide for 15 min at room temperature in the dark. Binding buffer was added, and apoptotic cells were detected by flow cytometoric analysis. To inhibit in vitro T cell apoptosis cocultured with PECs, PECs were treated with a Fas-Fc fusion protein (R&D Systems, Minneapolis, MN).

Confocal microscopic analysis

PECs including GFP^+ T cells were stained with PE-conjugated anti-CD11b mAb (eBioscience) on a glass slide. Coverslips were applied with Fluoromount-G (Molecular Probe). Cells were visualized using a Confocal Laser Microscan (LSM 5 Pascal; Carl Zeiss, Oberkochen, Germany).

Western blot analysis

Cell extracts from the nucleus and cytoplasm of $CD11b^+$ PECs were prepared using NE-PER Nuclear and Cytoplasmic Extraction Reagents (Thermo Fisher Scientific, Rockford, IL). A total of 10 μg of each sample per well was used for SDS-PAGE. After blocking with 5% nonfat milk, the membrane was incubated with primary Abs against phospho-IκBα and p50 (NF-κB1), RelA (p65), and histones (Santa Cruz Biotechnology, Santa Cruz, CA). Ag–Ab complexes were detected using HRP-conjugated secondary Abs. Protein binding was visualized using the Phototope-HRP Western blot Detection System (Cell Signaling Technology, Danvers, MA).

NF-κB transcription activity assay

The transcription activity of NF-κB in the nuclear extracts from PECs was analyzed with a NF-κB transcription factor colorimetric assay kit (Millipore, Billerica, MA). Briefly, nuclear extracts were incubated with a biotinylated double-stranded oligonucleotide probe containing the consensus sequence for NF-κB on a streptavidin-coated plate. Captured complexes, including active NF-κB protein, were incubated with the primary Abs for p50 and RelA. HRP-conjugated secondary Ab, and tetramethylbenzidine substrate. The absorbance of the samples was measured using a microplate reader at 450 nm.

Statistical analysis

Statistical significance was determined with an unpaired the Student *t* test.

Results

Normal T cell dynamics in Fas-deficient mice

To understand the dynamics of normal T cells in Fas-deficient mice, the T cells from GFP-TG mice were i.v. transferred into B6 and B6/*lpr* mice. On 7 d after the transfer, GFP^+ cells in the spleen and LNs of the recipient mice were analyzed. Although GFP^+ T cells were found in the spleen and LNs of B6 mice, these cells were barely detectable in B6/*lpr* mice (Fig. 1A). To evaluate the in vivo expansion of normal T cells in Fas-deficient mice using a homeostatic proliferation system, CFSE-labeled normal T cells from B6 mice were i.v. transferred into irradiated B6 and B6/*lpr* mice. On 7 d after the transfer, expanded T cells were found in B6 mice (Fig. 1B). However, the transferred $CFSE^+$ T cells in the spleen and LNs of B6/*lpr* mice were almost undetectable (Fig. 1B). In addition, to examine the in vivo Ag-specific T cell response in B6/*lpr* mice, $CD4^+$ T cells were purified from the spleen of OVA-specific TCR-TG (OT-II) mice and were transferred into B6 and B6/*lpr* mice. OVA peptide (100 μg/mouse) was injected into the recipient mice on the following day. On 7 d after the transfer, OT-II–specific $V\beta5.2^+CD4^+$ T cells of the spleen and LNs were analyzed. Although OT-II T cells were found in the spleen and LNs of B6 recipients, these cells were almost undetectable in the spleen and LNs of B6/*lpr* mice (Fig. 1C). These findings indicate that normal T cells fail to migrate to lymphoid tissues or survive under the Fas-deficient environment. In addition, we examined whether transferred T cells migrate to any specific organ other than lymphoid organs. On 7 d after the transfer of GFP-T cells, T cell diminishment was observed in the spleen, LNs, and liver of B6/*lpr* recipient mice (Fig. 1D). The accumulation of the donor T cells was not observed in any specific organs such as the lung, pancreas, and kidney. Furthermore, the donor T cells did not accumulate in the thymus, bone marrow, and PBMCs of B6/*lpr* recipient mice (Fig. 1D). These findings demonstrate that transferred normal T cells fail to survive in the lymphoid organs such as the spleen and LNs of B6/*lpr* recipients.

Migratory response of normal T cells in Fas-deficient recipients

To examine the migration of normal T cells to lymphoid tissues, in vivo imaging analysis of the dynamics of normal T cells in B6 and B6/*lpr* mice was performed. At 30 min after the transfer of

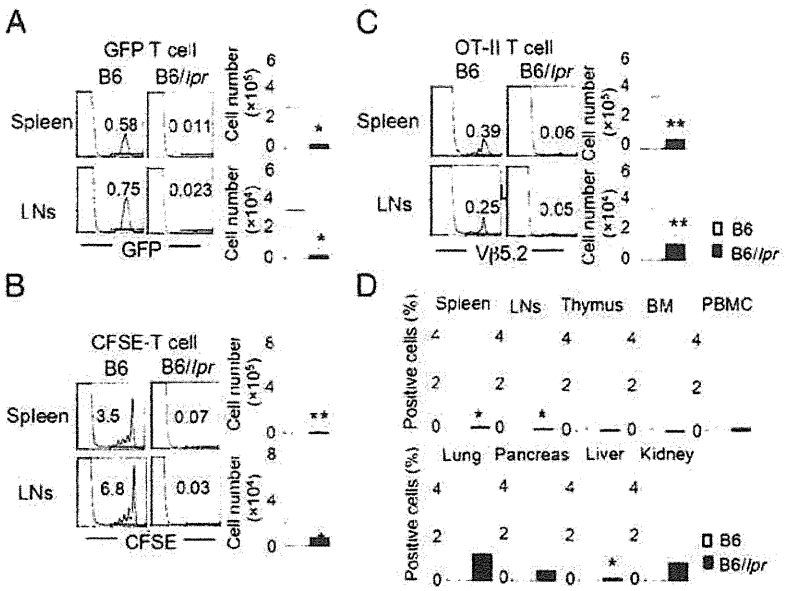

FIGURE 1. Dynamics of normal T cells in B6/*lpr* mice. (**A**) T cells (1×10^6) from GFP-TG mice were transferred into B6 and B6/*lpr* mice. GFP$^+$ T cells in the spleen and LNs of recipient mice at day 7 after the transfer were detected by flow cytometry. (**B**) CFSE-labeled T cells from B6 mice were transferred into irradiated (8.5 Gy) B6 and B6/*lpr* mice. CFSE$^+$ T cells in the spleen and LNs of recipient mice at day 7 after the transfer were detected by flow cytometry. (**C**) T cells (1×10^6) from OT-II mice were transferred into B6 and B6/*lpr* mice. Next day, OVA peptide was i.v. injected into the recipient mice. Vβ5.2$^+$CD4$^+$ T cells in the spleen and LNs of recipient mice at day 7 after the transfer were detected by flow cytometry. Cell numbers were compared between B6 and B6/*lpr* recipients ($n = 6$). (**D**) T cells from GFP-TG mice were transferred into B6 and B6/*lpr* mice. GFP$^+$ T cells in the spleen and LNs of recipient mice at day 7 after the transfer were detected by flow cytometry. GFP$^+$ cells (percentage) were shown as mean ± SD for five mice in each recipient group. $^*p < 0.05$, $^{**}p < 0.005$.

T cells. XenoLight DiR-labeled T cells were detected using an in vivo imaging analyzer. Although transferred T cells were detectable in the spleen of B6 and B6/*lpr* recipients, the fluorescence intensity in the spleen of B6/*lpr* recipients was considerably lower than that in the spleen of B6 recipients (Fig. 2A). This finding suggests that the transferred normal T cells were rapidly diminished in PBMCs before accumulating in lymphoid organs such as the spleen and LNs. In contrast, we have analyzed cell localization to the lung and liver after i.v. injection of T cells. Normal T cells were detectable in both *lpr* and control recipients, and there was no difference in T cell migration between *lpr* and control recipients (Supplemental Fig. 1). Moreover, when the transferred T cells (Thy1.1$^+$) were analyzed 30 min after the transfer, the rapid diminishment of T cells in B6/*lpr* recipients had already been observed (Fig. 2B). This suggests that rapid death and clearance of normal T cells may have occurred in the B6/*lpr* recipients immediately after the transfer. Moreover, when the Fas expression on the transferred normal T cells in B6 or B6/*lpr* recipients was analyzed 30 min after the transfer, significantly increased Fas expression was observed on the T cells in B6/*lpr* recipients compared with those in B6 recipients (Fig. 2C). Furthermore, when CFSE-labeled T cells from B6/*lpr* mice were i.v. injected into B6 and B6/*lpr* mice, the T cell diminishment was not detectable in both recipient mice (Fig. 2D). These results suggest that Fas expression on normal T cells plays a crucial role in the induction of rapid T cells diminishment in Fas-deficient recipients. These results imply that Fas-mediated cell death of normal T cells is enhanced in a Fas-deficient immune environment.

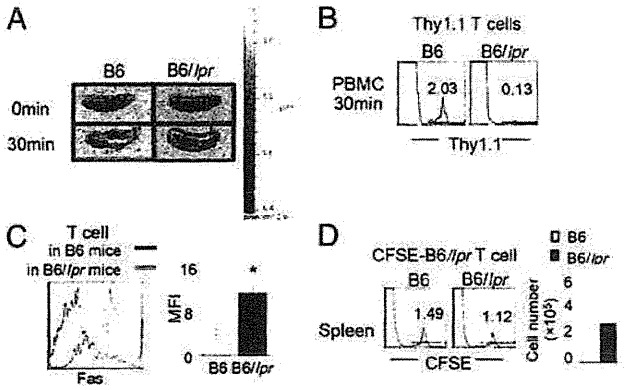

FIGURE 2. Rapid diminishment and Fas expression on the donor T cells in *lpr* recipients. (**A**) T cells (5×10^6) from B6 mice were labeled with XenoLight DiR and transferred into B6 and B6/*lpr* mice. The donor T cells in the spleen of the recipients 30 min after the transfer were detected using an in vivo imaging analyzer. Photos are representative of four mice in each recipient group. (**B**) T cells from B6 Thy1.1 mice were transferred into B6 and B6/*lpr* mice, and the donor T cells in PBMCs of the recipients 30 min after the transfer were detected by flow cytometry. Data are representative of five mice in each recipient group. (**C**) Cell surface Fas expression on the donor T cells in recipients was analyzed 30 min after the transfer by flow cytometry. Mean fluorescence intensity of Fas expression on donor T cells is shown as mean ± SD for five mice in each recipient group. $^*p < 0.05$. (**D**) CFSE-labeled T cells from B6/*lpr* mice were transferred into B6 and B6/*lpr* mice and detected at day 7 after transfer by flow cytometry. Data are representative of five mice in each recipient group.

FasL expression on immune cells in B6/lpr mice

Next, we analyzed FasL expression on peripheral immune cells in B6/*lpr* mice. When mRNA expression of FasL in the spleen of B6 and B6/*lpr* mice was analyzed by quantitative reverse transcription-PCR (RT-PCR), higher levels of FasL mRNA of all subsets including CD4$^+$ T cells, CD8$^+$ T cells, B220$^+$ B cells, CD11c$^+$ dendritic cells, and CD11b$^+$ macrophages were observed in B6/*lpr* mice compared with B6 mice (Fig. 3A). In addition, significantly increased FasL mRNA expression of subsets including CD4$^+$ T cells, CD8$^+$ T cells, and CD11b$^+$ macrophages was observed in PBMCs from B6/*lpr* mice compared with those of B6 mice (Fig. 3B). Therefore, we speculated that FasL–Fas-mediated apoptosis of normal T cells may be induced by the interaction with the peripheral immune cells in B6/*lpr* mice. In particular, because FasL mRNA expression on the CD11b$^+$ macrophages in the spleen and PBMCs of B6/*lpr* mice was much higher than that of B6 mice, macrophages may play a crucial role in T cell apoptosis and clearance in the immune system of B6/*lpr* mice. Thus, we focused on analyzing the macrophages in B6/*lpr* mice. When the surface expression of FasL on macrophages was analyzed by flow cytometry, the expression on the CD11b$^+$ macrophages of the PBMCs of B6/*lpr* mice was increased compared with that of B6 mice (Fig. 3C). These results suggest that increased FasL expressions on immune cells, including macrophages in a Fas-deficient immune condition, play an important

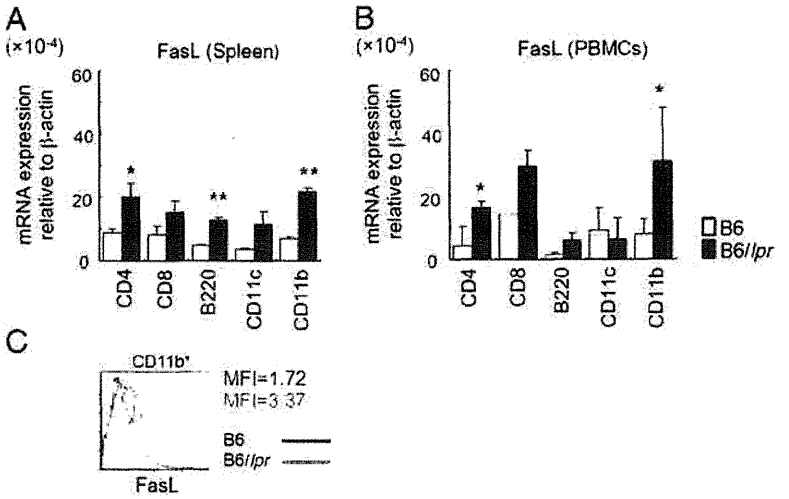

FIGURE 3. Enhanced expression of FasL on the immune cells in B6/*lpr* mice. (**A**) FasL mRNA expressions in spleen cells of B6 and B6/*lpr* mice were analyzed by quantitative RT-PCR. Data are shown as mean ± SD for five mice in each recipient group. $*p < 0.05$; $**p < 0.005$. (**B**) FasL mRNA expressions in PBMCs of B6 and B6/*lpr* mice were analyzed by quantitative RT-PCR. Data are shown as mean ± SD for five mice in each recipient group. $*p < 0.05$. (**C**) FasL expression on the CD11b$^+$ macrophages in PBMCs was detected by flow cytometry. Results are representative of three independent experiments.

role in the Fas-mediated rapid death of normal T cells in B6/*lpr* mice.

*Functions of macrophages in B6/*lpr *mice*

To understand the functions of the peripheral macrophages in B6/*lpr* mice, macrophages from thioglycolate-elicited PECs were used for analyzing their interaction with normal T cells. When the expression level of FasL on PECs was analyzed, significantly increased expression of FasL on PECs from B6/*lpr* mice was detected compared with B6 mice (Fig. 4A). Next, we examined whether in vitro T cell death was induced by coculture with PECs from B6/*lpr* mice. The proportion of apoptotic T cells cocultured with B6/*lpr* PECs was significantly enhanced compared with that of normal T cells cocultured with B6 PECs (Fig. 4B). To determine whether B6/*lpr* PECs engulf dead T cells rapidly, CFSE-labeled normal T cells were cocultured with CD11b$^+$ PECs for 3 h, and CD11b$^+$CFSE$^+$ macrophages engulfing apoptotic T cells were analyzed. We detected a significant increase of CFSE$^+$ CD11b$^+$ macrophages in B6/*lpr* mice compared with B6 mice (Fig. 4C). In addition, we investigated the phagocytic activity of B6/*lpr* macrophages with FITC-labeled latex beads. The phagocytic activity of CD11b$^+$ PECs in B6/*lpr* mice was significantly increased compared with that in B6 mice (Fig. 4D). To rule out that the apoptotic cells attached to macrophages, we fixed the macrophages after phagocytosis assay and then treated them with 0.01% Triton X-100. Because there was no change in the proportion of CD11b$^+$FITC$^+$ macrophages between before and after Triton X treatment, the macrophages engulfed, but not bound to, the beads in this assay (Supplemental Fig. 2). These results suggest that enhanced FasL expression on the macrophages in B6/*lpr* mice triggers the rapid cell death of normal T cells in a Fas-deficient immune environment, and increased phagocytic activity of B6/*lpr* macrophages plays a key role in the clearance of dead T cells.

In vivo functions of Fas-deficient macrophages

To determine the in vivo functions of macrophages in B6/*lpr* mice, normal T cells from GFP-TG mice were i.p. injected into the recipient mice that had been injected with thioglycolate. At 6 h after T cell injection, PECs including injected T cells were analyzed. Consistent with the results obtained from the i.v. injection of normal T cells into B6/*lpr* mice, the T cells injected (i.p.) into B6/*lpr* mice were significantly decreased compared with those injected into B6 mice (Fig. 5A). The number of apoptotic cells showing Annexin V$^+$ of injected T cells in B6/*lpr* mice was significantly higher compared with that in B6 mice (Fig. 5B). The depletion of T cells in B6/*lpr* recipients was inhibited by i.p. injection of anti-FasL mAb (Fig. 5C). Furthermore, when normal

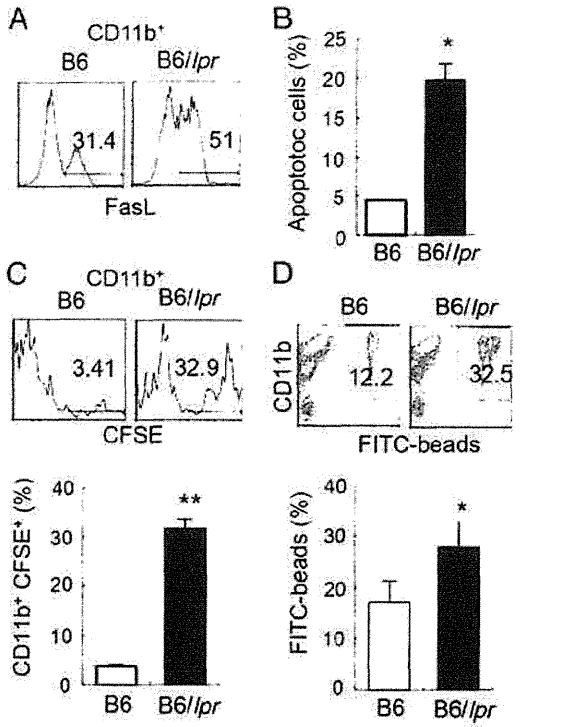

FIGURE 4. Enhanced FasL expression and phagocytotic activity of *lpr* macrophages in vitro. B6 and B6/*lpr* mice were i.p. injected with thioglycolate to obtain PECs. On day 4 after the injection, PECs were collected from peritoneal cavity. (**A**) FasL expression on CD11b$^+$ macrophages in PECs of B6 and B6/*lpr* mice was analyzed by flow cytometry. Data are representative of four independent experiments. (**B**) CFSE-labeled T cells from Thy1.1 B6 mice were cocultured with the CD11b$^+$ macrophages from PECs of B6 and B6/*lpr* mice. Annexin V$^+$ apoptotic T cells (percentage) are shown as mean ± SD for five mice in each group. $*p < 0.05$. (**C**) CFSE-labeled T cells from B6 mice were cocultured with the CD11b$^+$ macrophages from PECs of B6 and B6/*lpr* mice. Phagocytosis of CFSE$^+$ T cells by the CD11b$^+$ cells in PECs was evaluated by flow cytometry. Results are shown as mean ± SD for five mice in each group. $**p < 0.005$. (**D**) Phagocytic activity of CD11b$^+$ macrophages in PECs was evaluated by uptake of FITC-conjugated beads in vitro. Results are shown as mean ± SD for five mice in each group. $**p < 0.005$.

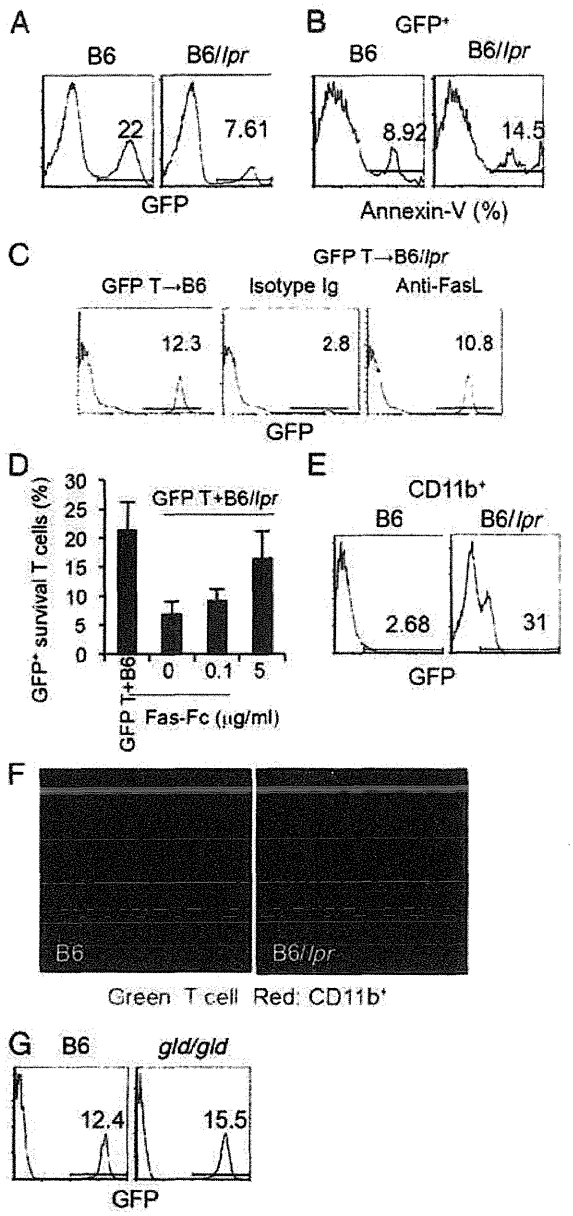

FIGURE 5. In vivo rapid death and phagocytosis of T cells by macrophages. (**A**) T cells (1×10^6) from GFP-TG mice were i.p. injected into the recipient mice treated with thioglycolate. GFP$^+$ T cells in PECs were detected by flow cytometry. Data are representative of four mice in each recipient group. (**B**) Annexin V$^+$ apoptotic cells (percentage) of GFP$^+$ T cells in PECs were detected by flow cytometry. Data are representative of four mice in each recipient group. (**C**) GFP T cells (1×10^6) were i.p. injected into thioglycolate-treated B6/*lpr* recipients together with anti-Fas mAb or isotype control Ig. (**D**) GFP T cells (5×10^4) were cocultured with B6/*lpr* PECs (2×10^5) fro 24 h in vitro in the presence of Fas-Fc fusion protein (0, 0.1, and 5 μg/ml). GFP$^+$ survival cells are shown as mean ± SD for triplicates. (**E**) Phagocytosis of GFP$^+$ T cells by the CD11b$^+$ macrophages in PECs was evaluated by flow cytometry. Data are representative of four mice in each recipient group. (**F**) GFP$^+$ T cells (green) and CD11b$^+$ macrophages (red) in PECs were detected by confocal microscopy. Original magnification ×630. Data are representative of four three independent experiments. (**G**) T cells from GFP-TG mice were i.p. injected into B6 and B6/*gld* mice treated with thioglycolate. GFP$^+$ T cells in PECs were detected by flow cytometry. Data are representative of four mice in each recipient group.

GFP-T cells were i.p. transferred into B6/*lpr* mice together with Fas-Fc fusion protein (0.1 and 5 μg/ml), survival T cells were significantly increased in comparison with those of the recipients without Fas-Fc (Fig. 5D). In addition, the phagocytic activity of CD11b$^+$ PECs in B6/*lpr* was significantly enhanced compared with that in B6/mice (Fig. 5E). Furthermore, microscopic analysis showed fewer normal T cells (GFP$^+$) in B6/*lpr* mice compared with B6 mice: moreover, it revealed phagocytic fragments of GFP$^+$ T cells within the macrophages in B6/*lpr* mice, although the fragments within the macrophages in B6 mice were undetectable (Fig. 5F). In contrast, when normal T cells from GFP-TG mice were i.p. injected into B6 and B6/*gld* mice, which are deficient in FasL expression, T cell diminishment was not observed (Fig. 5G). In contrast, we have performed the experiment using purified B cells. Because deletion of normal B cells in *lpr* recipients was not observed (Supplemental Fig. 3), T cell apoptosis may be closely associated with phagocytosis of *lpr* macrophages. Our findings reveal that Fas-deficient macrophages can induce rapid apoptosis through upregulated FasL and that Fas-deficient macrophages rapidly engulf apoptotic T cells.

Enhanced activation of Fas-deficient macrophages through NF-κB

NF-κB signaling plays a crucial role in the activation of macrophages (22, 23). Phosphorylation of IκBα, an endogenous inhibitory molecule of NF-κB activation by the interaction with NF-κB subunits, in CD11b$^+$PECs from B6/*lpr* mice was much higher than that in CD11b$^+$ PECs from B6 mice (Fig. 6A). Moreover, nuclear transport of NF κB subunits such as p50 and p65 in CD11b$^+$ PECs from B6/*lpr* mice was significantly enhanced compared with that in CD11b$^+$ PECs from B6 mice (Fig. 6A). In addition, the transcriptional activity of NF-κB in the nuclear protein of the CD11b$^+$ PECs from B6/*lpr* mice was significantly increased compared with that from B6 mice (Fig. 6B). In immune cells, including macrophages, there are several genes regulated by NF-κB such as TNF-α, IL-6, IL-1β, and FasL in immune cells including macrophage (24–27). The mRNA expression of TNF-α, IL-6, and IL-1β in CD11b$^+$ PECs from B6/*lpr* mice was not increased compared with that from B6 mice (Fig. 6C). In contrast, the FasL mRNA level in the CD11b$^+$ PECs from B6/*lpr* mice was significantly higher than that from B6 mice (Fig. 6D). When FasL mRNA of the CD11b$^+$ PECs from NF-κB$_1$ gene knockout mice bearing a *fas* gene mutant (*NF-κB$_1^{-/-}$/lpr*) was analyzed, the expression level was similar to that of B6 mice (Fig. 6D). Furthermore, the diminishment of normal T cells in *NF-κB$_1^{-/-}$/lpr* mice was not observed (Fig. 6E, 6F). These results suggest that FasL overexpression through NF-κB activation of macrophages is important for rapid T cell death in a Fas-deficient immune system.

Alteration of Fas expression on normal T cells in a Fas-deficient immune system

Fas expression is regulated by several factors or signaling pathways (28–31). One potent factor that induces Fas expression is IFN-γ (28). When the serum level of IFN-γ was analyzed by ELISA, we found that the concentration of the sera in B6/*lpr* mice was significantly higher compared with that in B6 mice (Fig. 7A). To determine the source of the high level of IFN-γ, subsets of peripheral immune cells including CD4$^+$ T cells, CD8$^+$ T cells, CD11b$^+$ macrophages, CD11c$^+$ dendritic cells, and B220$^+$ B cells in PBMCs were purified, and IFN-γ mRNA was analyzed by quantitative RT-PCR. The mRNA levels in CD4$^+$, CD8$^+$ T, and B220$^+$ B cells from B6/*lpr* mice increased significantly compared with those in B6 mice (Fig. 7B). When the T cells from normal mice or *IFNγR$^{-/-}$* mice were labeled with CFSE and were i.v. injected into B6/*lpr* mice, Fas expression on T cells in *IFNγR$^{-/-}$* mice was not enhanced, although the expression on T cells from B6 mice was considerably increased in Fas-deficient recipients

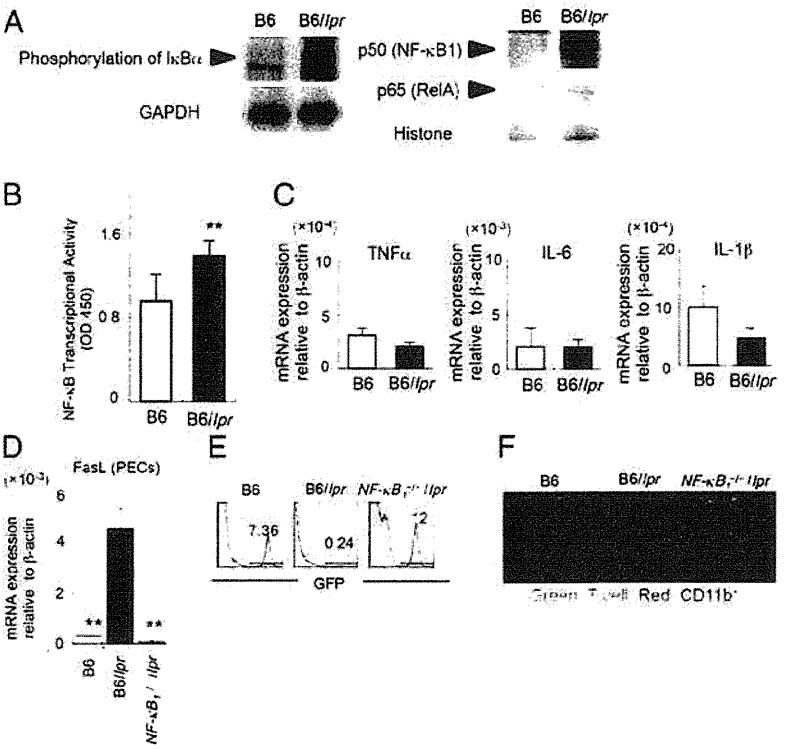

FIGURE 6. Control of FasL expression on *lpr* macrophages by NF-κB activation. **(A)** Phosphorylation of IκBα and nuclear translocation of the NF-κB subunits of $CD11b^+$ macrophages from thioglycolate-induced PECs were analyzed by Western blotting. GAPDH and histones were used as housekeeping proteins. Data are representative of three independent experiments. **(B)** Transcriptional activity of NF-κB in B6 and B6/*lpr* macrophages was detected. Results are shown as mean ± SD for five mice in each group. $^{**}p < 0.005$. **(C)** The mRNA expression of NF-κB–target genes was analyzed by quantitative RT-PCR. Data are shown as mean ± SD for five mice in each group. **(D)** FasL mRNA expression in the $CD11b^+$ macrophages from thioglycolate-induced PECs in B6, B6/*lpr*, and *NF-κB*$_1^{-/-}$/*lpr* mice was analyzed by quantitative RT-PCR. Data are shown as mean ± SD for five mice in each group. $^{**}p < 0.005$. **(E)** T cells from GFP-TG mice were i.p. injected into B6, B6/*lpr*, and *NF-κB*$_1^{-/-}$/*lpr* mice pretreated with thioglycolate. GFP^+ T cells in PECs were detected by flow cytometry. Data are representative of five mice in each group. **(F)** GFP^+ T cells (green) and $CD11b^+$ macrophages (red) in PECs were detected by confocal microscopy. Original magnification ×630. Photos are representative of four independent experiments.

(Fig. 7C). Fas expression on T cells was enhanced by recombinant IFN-γ in a dose-dependent manner (Supplemental Fig. 4). In addition, when T cells from *IFNγR*$^{-/-}$ mice were i.v. injected into B6/*lpr* mice, T cell diminishment, which had been observed in the Fas deficient recipients, was not detectable (Fig. 7D). Moreover, when T cells from *IFNγR*$^{-/-}$ mice were cocultured with *lpr* PECs, survival T cells of *IFNγR*$^{-/-}$ mice were significantly increased compared with those of wild-type mice (Fig. 7E). By the

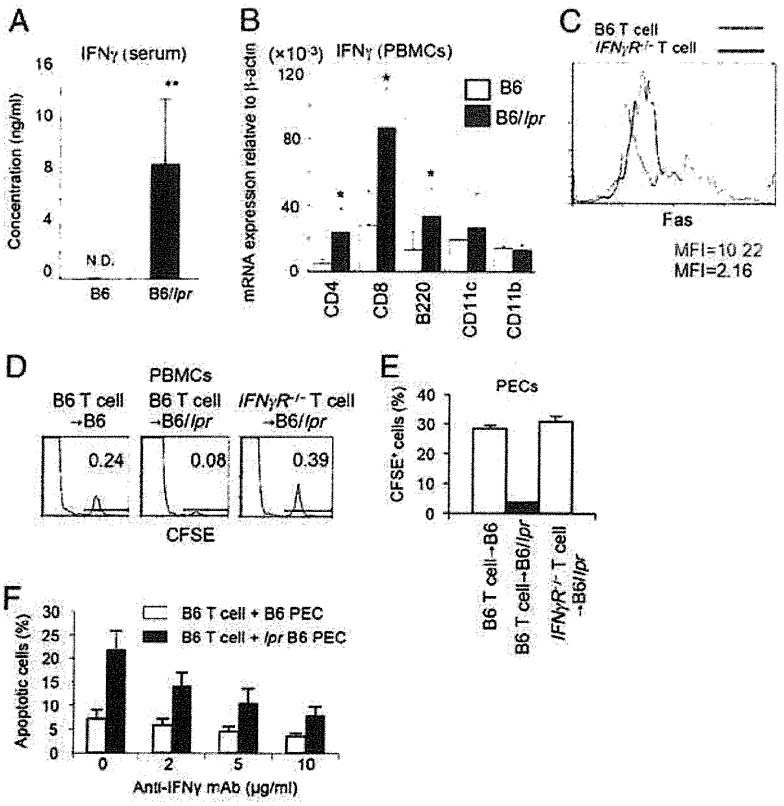

FIGURE 7. Regulation of Fas expression on donor T cells by IFN-γ in *lpr* mice. **(A)** Concentration of IFN-γ in the sera of B6 and B6/*lpr* mice was measured by ELISA. Results are shown as mean ± SD for six mice in each group. $^{**}p < 0.005$. **(B)** IFN-γ mRNA expressions in the subsets of spleen cells from B6 and B6/*lpr* mice were analyzed by quantitative RT-PCR. Results are shown as mean ± SD for five mice in each group. $^{*}p < 0.05$. **(C)** CFSE-labeled T cells from B6 and *IFNγR*$^{-/-}$ mice were i.v. injected into B6/*lpr* mice. Fas expression on the donor T cells in PBMCs of recipients was analyzed by flow cytometry. Data are representative of five mice in each group. Gray shadow shows isotype negative control. **(D)** CFSE-labeled T cells from B6 and *IFNγR*$^{-/-}$ mice were i.v. injected into B6 or B6/*lpr* mice and were detected by flow cytometry. Data are representative of four mice in each group. **(E)** CFSE-labeled T cells from B6 and *IFNγR*$^{-/-}$ mice were i.p. injected into thioglicolate-treated B6 or B6/*lpr* mice. $CFSE^+$ T cells in PECs were analyzed by flow cytometry. Results are shown as mean ± SD for four mice in each group. **(F)** T cells (2×10^4) from B6 mice were cocultured for 8 h with B6 or B6/*lpr* PECs (1×10^5) in the presence of anti–IFN-γ mAb (0, 2, 5, and 10 μg/ml). Apoptotic T cells were evaluated by flow cytometric analysis of expression of Annexin V. Results are shown as mean ± SD for triplicates in each group.

pretreatment of anti–IFN-γ mAb, apoptosis of normal activated T cell interacted with *lpr* PECs was inhibited in the dose-dependent manner (Fig. 7F). These findings suggest that the high level of IFN-γ in B6/*lpr* mice enhances Fas expression on injected normal T cells and that immune cells in B6/*lpr* mice highly expressing FasL induce Fas-mediated and rapid apoptosis of T cells.

Discussion

In this study, we confirmed that normal T cells failed to survive in a Fas-deficient immune condition using the transfer experiments. In addition, the homeostatic proliferation of T cells in lymphopenic recipients of *lpr* mice and Ag-specific T cell response in *lpr* mice were not observed. These findings are consistent with the results in the previous reports regarding the failure of normal lymphocyte survival in *lpr* hosts (17, 18). The phenomenon was thought to occur because of the induction of T cell apoptosis in *lpr* recipients because the transferred T cells did not migrate in any specific organs other than lymphoid tissues and the liver.

Because the diminishment of normal T cells was observed in PBMCs in 30 min immediately after the transfer, rapid death of transferred T cells may have occurred in *lpr* recipients. However, T cell diminishment in *lpr* donor mice was undetectable. Thus, the rapid T cell death occurred by the presence or absence of the Fas molecule on these cells.

Although enhanced FasL expression on immune cells in *lpr* mice has been described previously (18, 20), it was unclear as to which subset of immune cells in *lpr* mice overexpressed FasL molecule. In this study, mRNA expression of FasL of all subsets in the spleen and PBMCs of *lpr* mice was significantly higher than that of control mice. In particular, FasL mRNA expression in $CD11b^+$ macrophages in *lpr* mice was significantly increased compared with that in control mice. In addition, when thioglycolate elicited PECs, including a number of macrophages, were used to analyze the interaction with T cell in vivo and in vitro, enhanced rapid death and clearance of T cells by *lpr* macrophages was observed. Furthermore, phagocytic activity of *lpr* macrophages was considerably enhanced compared with control macrophages. These results suggest that *lpr* macrophages can phagocyte apoptotic T cells promptly as well as induce the rapid T cell death in the periphery. The *lpr* macrophages with enhanced expression of FasL may induce rapid death of T cells and promptly engulf the apoptotic cells by FasL-independent phagocytosis. There may be unknown cellular mechanism like "Eat me signal."

FasL, a type II transmembrane protein belonging to the TNF superfamily, is a well-characterized apoptosis initiating protein (32–34). Some transcription factors have been shown to regulate FasL gene expression, including specificity protein-1, IFN regulatory factor-1, NF in activated T cells and NF-κB (35–37). NF-κB plays key roles in differentiation and activation of macrophages (22, 38). Our results suggest that the direct contribution of macrophages to the induction of rapid death of T cells is very important for effective phagocytosis of apoptotic T cells. Furthermore, our results imply that the induction of expression of FasL in macrophages by NF-κB is negatively controlled by Fas signaling. This is related to our previous report that Fas signaling controls RANKL signaling following NF-κB activation in dendritic cells (39). Fas signaling may play important roles in NF-κB activation in relation to cell activation, survival, and growth in addition to apoptosis.

As to the relationship between FasL expression and phagocytosis in macrophages, it was reported that enhanced expression of FasL on Kupffer cells is associated with phagocytosis of apoptotic T cells in human liver allografts (40). Although further experiments will be needed to confirm the cellular mechanism, FasL-enhanced macrophages may engulf apoptotic cells effectively.

It is widely established that Fas expression on peripheral T cells plays a key role in AICD to maintain peripheral immune system (2, 3, 5). Fas expression on T cells increases by TCR signaling (41). In addition, some cytokines such as IL-2 and/or IFN-γ trigger the enhancement of Fas expression on T cells (42). Our results imply that an extremely high concentration of IFN-γ in the serum of *lpr* mice acts on the induction of Fas expression on the transferred T cells directly. When T cells from IFN-γR knockout mice were transferred into *lpr* mice, the rapid death and diminishment of T cells was not observed. These results strongly suggest that Fas expression on peripheral T cells is controlled through the IFN-γ/IFN-γR.

With regard to the control of the Fas expression of cells other than the T cell, it was reported that TNF-α can control the expression of fibroblasts in addition to IFN-γ (30). Although we found a high concentration of IFN-γ in the serum from *lpr* mice, the level of TNF-α concentration in the serum from *lpr* mice was similar to that from control mice (data not shown). In this study, when naive T cells from normal mice were transferred, they were not activated and slightly expressed the Fas molecule on the cell surface. Because of the exposure to the high concentration of IFN-γ in *lpr* mice, Fas expression on T cells rapidly increased. The immune cells highly expressing FasL including macrophages of *lpr* mice may induce the rapid apoptosis of T cells, and the macrophages in the peripheral immune system may rapidly phagocytize the apoptotic T cells.

In contrast, many reports indicate that B cells are maintained by Fas and Bim-dependent apoptosis to protect autoimmunity (43–45). In our experiment, $CD19^+$ B cells failed to undergo apoptosis in Fas-deficient host, although FasL expression on immune cells was enhanced. This finding implies that rapid T cell death may be triggered by cell–cell contact between normal T cells and Fas-deficient macrophages through the interaction with cell surface molecules such as MHC class II, costimulatory molecules, or TCR, although its precise mechanism has been still clarified.

Our results suggest that Fas signaling contributes to nonapoptotic functions such as the phagocytic activity of macrophages. Fas promotes the differentiation, proliferation, and maturation in several cells (1, 2, 46). Fas-associated death domain–mediated activation of caspase 8 is essential for the process of apoptosis of various cells (12, 47). In addition, it was reported that Rho GTPase Rac1 sensitizes T cells to Fas-induced apoptosis correlated with Rac-mediated cytoskeletal reorganization, dephosphorylation of the ezrin/radixin/moesin family of cytoskeletal linker proteins, and the translocation of Fas to lipid raft microdomain (48). However, the molecular mechanism for controlling the phagocytic activity of macrophages through Fas signaling has yet to be elucidated.

Although it has been reported that normal immune cells failed to survive in *lpr* recipients, the precise mechanism for its phenomenon remained unclear. In this study, we found that abnormal macrophages in *lpr* mice play critical roles in the disorder of the peripheral immune system. Our findings are thought to be important for therapeutic strategies for immune disorders such as ALPS or the other autoimmune diseases related to the abnormal expression of Fas on immune cells. In addition, this study suggests that Fas expression on macrophages contributes to the survival of T cells in the peripheral immune system. Taken together, this study strongly suggests that Fas-expressing macrophages play a pivotal role in maintaining T cell homeostasis in addition to AICD in the periphery.

Acknowledgments

We thank S. Katada, A. Katayama, and N. Kino for technical assistance.

Disclosures

The authors have no financial conflicts of interest.

References

1. Nagata, S. 1997. Apoptosis by death factor. *Cell* 88: 355–365.
2. Krammer, P. H. 2000. CD95's deadly mission in the immune system. *Nature* 407: 789–795.
3. Strasser, A., P. J. Jost, and S. Nagata. 2009. The many roles of FAS receptor signaling in the immune system. *Immunity* 30: 180–192.
4. Alderson, M. R., T. W. Tough, T. Davis-Smith, S. Braddy, B. Falk, K. A. Schooley, R. G. Goodwin, C. A. Smith, F. Ramsdell, and D. H. Lynch. 1995. Fas ligand mediates activation-induced cell death in human T lymphocytes. *J. Exp. Med.* 181: 71–77.
5. Maher, S., D. Toomey, C. Condron, and D. Bouchier-Hayes. 2002. Activation-induced cell death: the controversial role of Fas and Fas ligand in immune privilege and tumour counterattack. *Immunol. Cell Biol.* 80: 131–137.
6. Zhang, J., X. Xu, and Y. Liu. 2004. Activation-induced cell death in T cells and autoimmunity. *Cell. Mol. Immunol.* 1: 186–192.
7. Shultz, L. D., and C. L. Sidman. 1987. Genetically determined murine models of immunodeficiency. *Annu. Rev. Immunol.* 5: 367–403.
8. Jabs, D. A., and R. A. Prendergast. 1988. Murine models of Sjögren's syndrome: immunohistologic analysis of different strains. *Invest. Ophthalmol. Vis. Sci.* 29: 1437–1443.
9. Cohen, P. L., and R. A. Eisenberg. 1991. Lpr and gld: single gene models of systemic autoimmunity and lymphoproliferative disease. *Annu. Rev. Immunol.* 9: 243–269.
10. Kotzin, B. L. 1996. Systemic lupus erythematosus. *Cell* 85: 303–306.
11. Singer, P. A., and A. N. Theofilopoulos. 1990. Novel origin of lpr and gld cells and possible implications in autoimmunity. *J. Autoimmun.* 3: 123–135.
12. Boldin, M. P., E. E. Varfolomeev, Z. Pancer, I. L. Mett, J. H. Camonis, and D. Wallach. 1995. A novel protein that interacts with the death domain of Fas/APO1 contains a sequence motif related to the death domain. *J. Biol. Chem.* 270: 7795–7798.
13. Scaffidi, C., S. Fulda, A. Srinivasan, C. Friesen, F. Li, K. J. Tomaselli, K. M. Debatin, P. H. Krammer, and M. E. Peter. 1998. Two CD95 (APO-1/Fas) signaling pathways. *EMBO J.* 17: 1675–1687.
14. Curtin, J. F., and T. G. Cotter. 2003. Live and let die: regulatory mechanisms in Fas-mediated apoptosis. *Cell. Signal.* 15: 983–992.
15. Hughes, P. D., G. T. Belz, K. A. Fortner, R. C. Budd, A. Strasser, and P. Bouillet. 2008. Apoptosis regulators Fas and Bim cooperate in shutdown of chronic immune responses and prevention of autoimmunity. *Immunity* 28: 197–205.
16. Green, D. R., and M. Schuler. 2000. T cell development: some cells get all the breaks. *Nat. Immunol.* 1: 15–17.
17. Ettinger, R., J. K. Wang, P. Bossu, K. Papas, C. L. Sidman, A. K. Abbas, and A. Marshak-Rothstein. 1994. Functional distinctions between MRL-lpr and MRL-gld lymphocytes: normal cells reverse the gld but not lpr immunoregulatory defect. *J. Immunol.* 152: 1557–1568.
18. Wei, Y., K. Chen, G. C. Sharp, and H. Braley-Mullen. 2004. Fas ligand is required for resolution of granulomatous experimental autoimmune thyroiditis. *J. Immunol.* 173: 7615–7621.
19. Theofilopoulos, A. N., R. S. Balderas, Y. Gozes, M. T. Aguado, L. M. Hang, P. R. Morrow, and F. J. Dixon. 1985. Association of lpr gene with graft-vs.-host disease-like syndrome. *J. Exp. Med.* 162: 1–18.
20. Chu, J. L., P. Ramos, A. Rosendorff, J. Nikolić-Zugić, E. Lacy, A. Matsuzawa, and K. B. Elkon. 1995. Massive upregulation of the Fas ligand in lpr and gld mice: implications for Fas regulation and the graft-versus-host disease-like wasting syndrome. *J. Exp. Med.* 181: 393–398.
21. Allison, J., and A. Strasser. 1998. Mechanisms of β cell death in diabetes: a minor role for CD95. *Proc. Natl. Acad. Sci. USA* 95: 13818–13822.
22. Hawiger, J. 2001. Innate immunity and inflammation: a transcriptional paradigm. *Immunol. Res.* 23: 99–109.
23. Spehlmann, M. E., and L. Eckmann. 2009. Nuclear factor-κB in intestinal protection and destruction. *Curr. Opin. Gastroenterol.* 25: 92–99.
24. Dunn, S. M., L. S. Coles, R. K. Lang, S. Gerondakis, M. A. Vadas, and M. F. Shannon. 1994. Requirement for nuclear factor (NF)-κB p65 and NF-interleukin-6 binding elements in the tumor necrosis factor response region of the granulocyte colony-stimulating factor promoter. *Blood* 83: 2469–2479.
25. Baer, M., A. Dillner, R. C. Schwartz, C. Sedon, S. Nedospasov, and P. F. Johnson. 1998. Tumor necrosis factor α transcription in macrophages is attenuated by an autocrine factor that preferentially induces NF κB p50. *Mol. Cell. Biol.* 18: 5678–5689.
26. Mercurio, F., and A. M. Manning. 1999. Multiple signals converging on NF-κB. *Curr. Opin. Cell Biol.* 11: 226–232.
27. Torgler, R., S. Jakob, E. Ontsouka, U. Naehbur, C. Mueller, D. R. Green, and T. Brunner. 2004. Regulation of activation-induced Fas (CD95/Apo-1) ligand expression in T cells by the cyclin B1/Cdk1 complex. *J. Biol. Chem.* 279: 37334–37342.
28. Nagafuji, K., T. Shibuya, M. Harada, S. Mizuno, K. Takenaka, T. Miyamoto, T. Okamura, H. Gondo, and Y. Niho. 1995. Functional expression of Fas antigen (CD95) on hematopoietic progenitor cells. *Blood* 86: 883–889.
29. De Maria, R., and R. Testi. 1998. Fas-FasL interactions: a common pathogenetic mechanism in organ-specific autoimmunity. *Immunol. Today* 19: 121–125.
30. Frankel, S. K., G. P. Cosgrove, S. I. Cha, C. D. Cool, M. W. Wynes, B. L. Edelman, K. K. Brown, and D. W. Riches. 2006. TNF α sensitizes normal and fibrotic human lung fibroblasts to Fas-induced apoptosis. *Am. J. Respir. Cell Mol. Biol.* 34: 293–304.
31. Wynes, M. W., B. L. Edelman, A. G. Kostyk, M. G. Edwards, C. Coldren, S. D. Groshong, G. P. Cosgrove, E. F. Redente, A. Bamberg, K. K. Brown, et al. 2011. Increased cell surface Fas expression is necessary and sufficient to sensitize lung fibroblasts to Fas ligation-induced apoptosis: implications for fibroblast accumulation in idiopathic pulmonary fibrosis. *J. Immunol.* 187: 527–537.
32. Ju, S. T., D. J. Panka, H. Cui, R. Ettinger, M. el-Khatib, D. H. Sherr, B. Z. Stanger, and A. Marshak-Rothstein. 1995. Fas(CD95)/FasL interactions required for programmed cell death after T-cell activation. *Nature* 373: 444–448.
33. Janssen, O., J. Qian, A. Linkermann, and D. Kabelitz. 2003. CD95 ligand—death factor and costimulatory molecule? *Cell Death Differ.* 10: 1215–1225.
34. Lettau, M., M. Paulsen, H. Schmidt, and O. Janssen. 2011. Insights into the molecular regulation of FasL (CD178) biology. *Eur. J. Cell Biol.* 90: 456–466.
35. Chow, W. A., J. J. Fang, and J. K. Yee. 2000. The IFN regulatory factor family participates in regulation of Fas ligand gene expression in T cells. *J. Immunol.* 164: 3512–3518.
36. Jayanthi, S., X. Deng, B. Ladenheim, M. T. McCoy, A. Cluster, N. S. Cai, and J. L. Cadet. 2005. Calcineurin/NFAT-induced up-regulation of the Fas ligand/Fas death pathway is involved in methamphetamine-induced neuronal apoptosis. *Proc. Natl. Acad. Sci. USA* 102: 868–873.
37. Yao, P. L., Y. C. Lin, P. Sawhney, and J. H. Richburg. 2007. Transcriptional regulation of FasL expression and participation of sTNF-α in response to sertoli cell injury. *J. Biol. Chem.* 282: 5420–5431.
38. Lawrence, T., and G. Natoli. 2011. Transcriptional regulation of macrophage polarization: enabling diversity with identity. *Nat. Rev. Immunol.* 11: 750–761.
39. Izawa, T., N. Ishimaru, K. Moriyama, M. Kohashi, R. Arakaki, and Y. Hayashi. 2007. Crosstalk between RANKL and Fas signaling in dendritic cells controls immune tolerance. *Blood* 110: 242–250.
40. Miyagawa-Hayashino, A., T. Tsuruyama, H. Egawa, H. Haga, H. Sakashita, T. Okuno, S. Toyokuni, K. Tamaki, H. Yamabe, T. Manabe, and S. Uemoto. 2007. FasL expression in hepatic antigen presenting cells and phagocytosis of apoptotic T cells by FasL+ kupffer cells are indicators of rejection activity in human liver allografts. *Am. J. Pathol.* 177: 1499–1508.
41. Marrack, P., and J. Kappler. 2004. Control of T cell viability. *Annu. Rev. Immunol.* 22: 765–787.
42. Carter, L. L., X. Zhang, C. Dubey, P. Rogers, L. Tsui, and S. L. Swain. 1998. Regulation of T cell subsets from naive to memory. *J. Immunother.* 21: 181–187.
43. Hutcheson, J., J. C. Scatizzi, A. M. Siddiqui, G. K. Haines, III, T. Wu, Q. Z. Li, L. S. Davis, C. Mohan, and H. Perlman. 2008. Combined deficiency of proapoptotic regulators Bim and Fas results in the early onset of systemic autoimmunity. *Immunity* 28: 206–217.
44. Bouillet, P., D. Metcalf, D. C. Huang, D. M. Tarlinton, T. W. Kay, F. Köntgen, J. M. Adams, and A. Strasser. 1999. Proapoptotic Bcl-2 relative Bim required for certain apoptotic responses, leukocyte homeostasis, and to preclude autoimmunity. *Science* 286: 1735–1738.
45. Enders, A., P. Bouillet, H. Puthalakath, Y. Xu, D. M. Tarlinton, and A. Strasser. 2003. Loss of the pro-apoptotic BH3-only Bcl-2 family member Bim inhibits BCR stimulation-induced apoptosis and deletion of autoreactive B cells. *J. Exp. Med.* 198: 1119–1126.
46. Peter, M. E., R. C. Budd, J. Desbarats, S. M. Hedrick, A. O. Hueber, M. K. Newell, L. B. Owen, R. M. Pope, J. Tschopp, H. Wajant, et al. 2007. The CD95 receptor: apoptosis revisited. *Cell* 129: 447–450.
47. Muzio, M., A. M. Chinnaiyan, F. C. Kischkel, K. O'Rourke, A. Shevchenko, J. Ni, C. Scaffidi, J. D. Bretz, M. Zhang, R. Gentz, et al. 1996. FLICE, a novel FADD-homologous ICE/CED-3-like protease, is recruited to the CD95 (Fas/APO-1) death- inducing signaling complex. *Cell* 85: 817–827.
48. Ramaswamy, M., C. Dumont, A. C. Cruz, J. R. Muppidi, T. S. Gomez, D. D. Billadeau, V. L. Tybulewicz, and R. M. Siegel. 2007. Cutting edge: Rac GTPases sensitize activated T cells to die via Fas. *J. Immunol.* 179: 6384–6388.

Unique Roles of Estrogen-Dependent Pten Control in Epithelial Cell Homeostasis of Mouse Vagina

Shinichi Miyagawa[1], Masaru Sato[1], Tamotsu Sudo[2], Gen Yamada[3], Taisen Iguchi[1,*]

[1]Okazaki Institute for Integrative Bioscience, National Institute for Basic Biology, National Institutes of Natural Sciences, and Department of Basic Biology, The Graduate University for Advanced Studies, Okazaki, Aichi 444-8787, Japan

[2]Section of Translational Research and Department of Gynecologic Oncology, Hyogo Cancer Center, Akashi, Hyogo 673-8558, Japan

[3]Department of Developmental Genetics and Laboratory Animal Center, Institute of Advanced Medicine, Wakayama Medical University, Wakayama, Wakayama 641-8509, Japan

*Correspondence: Taisen Iguchi, National Institute for Basic Biology, Okazaki 444-8787, Japan
E-mail: taisen@nibb.ac.jp
Phone: +81-564-59-5235, Fax: +81-564-59-5236

Keywords: Vagina, Pten, Akt, Estrogen, Epithelium

Short title: Pten function in vagina

25

26 **Abbreviations;** Akt, v-akt murine thymoma viral oncogene homolog; CAH; complex
27 atypical hyperplasia, CK; cytokeratin, CKO; conditional knock-out, E2, 17β-estradiol;
28 EGF, epidermal growth factor; ER, estrogen receptor; IGF, insulin-like growth factor,
29 MAPK, mitogen-activated protein kinase; mTOR, mammalian target of rapamycin;
30 OVX, ovariectomy; PI3K, phosphoinositide-3-kinase; PTEN, phosphatase and tensin
31 homolog deleted from chromosome 10; PIP_3, phosphatidylinositol 3,4,5-trisphosphate;
32 PIP_2, phosphatidylinositol 4,5-bisphosphate

33

Abstract

Numerous studies support a role of Phosphatase and tensin homolog deleted from chromosome 10 (Pten) as a tumor suppressor gene that controls epithelial cell homeostasis to prevent tumor formation. Mouse vaginal epithelium cyclically exhibits cell proliferation and differentiation in response to estrogen and provides a unique model for analyzing homeostasis of stratified squamous epithelia. We analyzed vaginal epithelium-specific *Pten* conditional knock-out (CKO) mice to provide new insights into Pten/phosphoinositide-3-kinase (PI3K)/Akt function. The vaginal epithelium of ovariectomized (OVX) mice (control) was composed of 1-2 layers of cuboidal cells, while OVX CKO mice exhibited epithelial hyperplasia in the suprabasal cells with increased cell mass and mucin production. This is possibly due to misactivation of mammalian target of rapamycin (mTOR) and mitogen-activated protein kinase (MAPK). Intriguingly, estrogen administration to OVX *Pten* CKO mice induced stratification and keratinized differentiation in the vaginal epithelium as in estrogen-treated controls. We found Pten is exclusively expressed in the suprabasal cells in the absence of estrogens, whereas estrogen administration induced Pten expression in the basal cells. This suggests that Pten acts to prevent excessive cell proliferation as in the case for other squamous tissues. Thus, Pten exhibits a dual role on the control of vaginal homeostasis, dependent on whether estrogens are present or absent. Our results provide new insights into how Pten functions in tissue homeostasis.

Introduction

Phosphatase and tensin homolog deleted from chromosome 10 (Pten) is a lipid phosphatase that functions as a tumor-suppressor, and mutations in Pten are frequently found both in sporadic and hereditary cancers. Pten acts in opposition to phosphatidylinositol 3-kinase (PI3K) function. In the absence of Pten activity, concentrations of phosphatidylinositol 3,4,5-trisphosphate (PIP_3), a lipid second messenger produced by PI3K, are increased, leading to enhancement of phosphorylation and activation of the v-akt murine thymoma viral oncogene homolog (Akt). Akt kinase activity exerts anti-apoptotic and pro-proliferative functions; therefore, mice with *Pten* deletion and/or loss-of-function mutations are highly susceptible to tumor induction by abnormal Akt activation. Pten plays a pivotal role in maintaining stratified squamous epithelia because conditional knockout of *Pten* in the epithelium leads to hyperplasia, hyperkeratosis, and tumor formation in skin, esophagus and stomach [1].

Cell proliferation and differentiation of stratified squamous epithelia must be tightly regulated and coordinated during homeostasis. Vaginal epithelium, despite its similarity to other stratified squamous epithelia, is exceptional in one major way - the vaginal epithelium exhibits cyclical, estrogen-dependent cell proliferation and differentiation during the estrous cycle. The vaginae of ovariectomized (OVX) mice contain an atrophied epithelium of 2-3 cell layers; estrogen administration rapidly induces epithelial cell proliferation in the basal layer. The suprabasal cells are no longer mitogenic but differentiate while moving up through the epithelium. Apical cells exhibit keratinization. The fully stratified and keratinized vaginal epithelium resembles the typical stratified and keratinized epidermis found in the skin and other organs. Thus, the vaginal epithelium provides a unique model to study homeostasis in stratified squamous

79 epithelia. There are several case reports of vaginal cysts in the patients with Cowden's
80 disease, which is associated with *Pten* mutation [2,3]. In addition, there is one reported
81 description of a vaginal squamous cell carcinoma in *Pten* mutant mice [4]. However, little
82 is known about the usual function of Pten/PI3K/Akt signaling or its relationship with
83 estrogen signaling in the vagina.
84 In rodent reproductive organs such as vagina and uterus, the effects of
85 estrogen on the epithelia are mediated primarily via stromally expressed estrogen
86 receptor α (ERα) [5,6]. Estrogen-induced growth factors secreted from the stroma
87 promote epithelial cell proliferation [7], resulting in activation of cellular signal
88 transduction via PI3K/Akt and mitogen-activated protein kinase (MAPK) signaling
89 cascades [8,9]. Epidermal growth factor (EGF)-like growth factors and insulin-like growth
90 factor (IGF)-I have mitogenic effects similar to estrogens and administration of these
91 growth factors to OVX adult mice induced cell proliferation and differentiation in the
92 female reproductive tract [10-12]. These results suggest that Akt and MAPK signalings are
93 functional mediators of estrogen-induced cell proliferation and differentiation.
94 Importantly, aberrant PI3K/Akt activation results in complex atypical hyperplasia and
95 endometrioid carcinoma in the uterus [13-16]. Therefore, repression of PI3K/Akt signaling
96 is considered to be essential during the absence of estrogen in the vagina as well.
97 In the present study, we analyzed epithelium-specific *Pten* conditional
98 knock-out (CKO) mouse vagina to provide new insights into Pten/PI3K/Akt function.
99 We found that Pten is expressed in suprabasal epithelial cells where it prevents
100 abnormal cell proliferation and differentiation in the absence of estrogen. On the other
101 hand, in the presence of estrogen, Pten is predominantly expressed in basal epithelial
102 cells, where it may aid in preventing tumor induction. Thus, Pten exhibits a dual role on

the control of vaginal homeostasis, depending on the presence and absence of estrogen.

105 **Results**

106 *Effect of epithelial cell-specific inactivation of Pten on the mouse vagina*

107 CK5 is generally expressed in the stratified and squamous epithelium [17].
108 Hence, *Pten* CKO induced by *CK5*-Cre-mediated deletion progressively developed
109 hyperplasia and keratosis in the stratified and keratinized organs, which include
110 epidermis of the skin, tongue, esophagus and forestomach (Fig. S1). We first explored
111 whether *Pten* CKO induced hyperplasia and/or hyperkeratinization in the vagina as well.
112 The epithelial cell-specific expression of Cre in the *K5-Cre* line was confirmed Rosa
113 reporter mouse (Fig. S2). Accordingly, the epithelium-specific deletion of *Pten* was
114 evident in the *Pten* CKO mouse vagina (Fig. 1; Note that stromally expressed Pten is
115 still evident). In the current study, OVX mice were used to avoid any effects of
116 hypothalamus-pituitary-gonadal axis, and to simply analyze the effects of
117 Pten/PI3K/Akt in the absence of estrogen signaling (all information for intact *Pten* CKO
118 phenotypes are included in Fig. S3).

119 The vaginal epithelium of 8-week-old ovariectomized (OVX) mice (control)
120 was composed of 1-2 layers of cuboidal cells (Fig. 2A). In the CKO mice, epithelial
121 hyperplasia was evident, which was accompanied with distended cells in the superficial
122 layer of the vagina (Fig. 2B, B'). We also found multiple abnormal gland-like pits in the
123 epithelium. The epithelial cells lining the pits were positive for PAS and Alcian blue
124 staining (Fig. 2C-F), indicating mucin production. Such mucin production was observed
125 restrictedly in the superficial layer of cells, but not in the basal cells, of the vaginal
126 epithelium. PAS and Alcian blue positive cells were limited in the superficial layer of
127 the control vaginae. Thus, the phenotypes of *Pten* CKO mice probably result from
128 defects in the control of epithelial cell proliferation and differentiation, causing

129 increased mucin production in epithelial cells. Intriguingly, E2 administration in *Pten*
130 CKO mice induced stratification and keratinized differentiation in the vaginal
131 epithelium comparable to that in E2-treated controls (Fig. 2G, H). The epithelium in the
132 *Pten* CKO mice administrated with E2 is thicker than that of controls (Fig. 2I). PAS and
133 Alcian blue positive cells were not observed in E2-treated control or *Pten* CKO mouse
134 vagina (data not shown). At 2 weeks after the last E2 administration, *Pten* CKO mouse
135 vaginae exhibited a recurrence of the abnormal phenotypes (Fig. 2J), thus the vaginal
136 changes in the *Pten* CKO mouse are dependent on the absence of estrogen. We also
137 investigated the effects of a prolonged E2 exposure. Two months after implantation with
138 E2 pellet, *Pten* CKO mice exhibited frequent invagination of the vaginal epithelium into
139 underlying stroma (Fig. 2K, L), which might be associated with tumor formation later in
140 life [4].
141
142 *Cell differentiation in the Pten* CKO *mouse vaginal epithelial cells*
143 To further characterize the phenotypes of the *Pten* CKO mouse vagina,
144 several immunohistochemical stainings were performed. CK14 is a whole epithelial
145 marker in the vagina [18]. In both control and *Pten* CKO mice, CK14 was expressed
146 throughout all layers of the vaginal epithelium (Fig. 3A, B). In the control OVX mice,
147 the stratified and squamous differentiation marker, CK1 was expressed in several
148 suprabasal cells, whereas its expression was not observed in the OVX *Pten* CKO mice
149 (Fig. 3C, D). CK8 is a marker for undifferentiated cells and was expressed in some
150 suprabasal cells in the control OVX mouse vaginae (Fig. 3E). Intriguingly, CK8 was
151 strongly expressed in the OVX *Pten* CKO mouse vagina (Fig. 3F). We infer from these
152 results that suprabasal cells in the *Pten* CKO mouse vaginae are maintained an

153 undifferentiated, proliferating state. p63 is normally expressed in the basal layer of the
154 epithelium and is a crucial regulator of squamous differentiation [19, 20]. p63 was
155 expressed in cells adjacent to the basement membrane in OVX control mice, whereas its
156 expression in OVX *Pten* CKO mice was not restricted in the basal cells and was
157 observed some suprabasal cells away from the basement membrane (Fig. 3G, H).
158 After E2-administration, these marker proteins were similarly expressed in
159 both control and the mutant mouse vagina (Fig. 3I-N), but p63 expression in mutant
160 animals was more extensive in the upper layers (Fig. 3O, P).
161
162 *Cell proliferation, but not apoptosis is increased in the Pten* CKO *mouse vaginae*
163 We next investigated the proliferation indices of vaginal epithelial cells in
164 control and *Pten* CKO mice using BrdU incorporation. Proliferation indices were higher
165 in the OVX CKO than in OVX controls (Fig. 4A, B, E). In both control and mutants,
166 BrdU-positive cells were mostly found adjacent to or attached to the basement
167 membrane but some cells in the upper layer were positive for BrdU staining (red
168 arrowheads in Fig. 4B) in the *Pten* CKO mouse vagina. Three-successive
169 administrations of E2 strongly stimulated cell proliferation in both control and *Pten*
170 CKO mice (Fig. 4C, D, E).
171 We also examined whether reduced apoptosis in the epithelial cell contributed
172 to the phenotypes in the *Pten* CKO mouse vagina. Apoptotic indices as measured by
173 TUNEL staining did not differ significantly between control and mutant vaginal
174 epithelia (Fig. 4F-H). Apoptotic cells were almost undetectable in the vagina of E2
175 treated control and mutant mice (data not shown). These results indicate that *Pten*
176 loss-of-function enhanced cell proliferation in the OVX mice but not significantly alter

177 apoptosis.

178

179 *Activation of mTOR and MAPK pathway in the mutants*

180 To identify potential molecular mechanisms that could lead to abnormal cell
181 proliferation and differentiation in the vaginal epithelium, we examined
182 phosphorylation levels of known downstream effector of the Akt signaling pathway,
183 mammalian target of rapamycin (mTOR) [21-23]. As expected, enhanced Akt
184 phosphorylation was observed in the mutant mouse vagina (Fig. 5A, B). In addition,
185 mTOR phosphorylation was significantly increased in Pten mutant vaginae (Fig. 5A, B).
186 To explore the contribution of mTOR to the mutant phenotype, rapamycin, a specific
187 inhibitor of mTOR, was administrated to control and *Pten* CKO OVX mice. Rapamycin
188 administration for 3 weeks resulted in regression of cells in the suprabasal layer of most
189 part of the vagina, although mucus-like products still remained (Fig. 5C-F). Levels of
190 cell proliferation in mutant rapamycin-treated group were slightly increased compared
191 to control rapamycin-treated mice (Fig. 5G). Importantly, the index in the mutants with
192 rapamycin was reduced by half (5.1% vs. 10.3%), compared with that of OVX *Pten*
193 CKO mice without rapamycin (Fig. 5G). Rapamycin administration did not influence
194 on the Akt phosphorylation (Fig. 5H), indicating specific inhibition of mTOR complex
195 1 pathway. These results indicate that increased cell proliferation in *Pten* mutant vaginal
196 epithelium at least partly requires the mTOR pathway.

197 Activation of MAPK has been implicated for mucin production in the
198 respiratory tract, intestine and prostate [24-26]. Indeed, we observed increased expression
199 of phosphorylated mitogen-activated protein kinase (MEK) and extracellular
200 signal-regulated kinase (ERK1/2) in the suprabasal cells from *Pten* CKO animals (Fig.

201 6A-D). Activated MAPK remained in the *Pten* CKO mice administrated with rapamycin
202 (Fig. 6E, F), supporting the fact that rapamycin did not repress mucin production (Fig.
203 5D, F).
204 It is known that activated MAPK and/or Akt can stimulate the transcriptional
205 activity of ERα (in a ligand-independent manner) by phosphorylating serines 118 and
206 167 of this receptor (located within the AF-1 region), respectively [27-29]. ERα protein
207 was observed in the vaginal epithelium and stroma of both control and *Pten* CKO
208 animals (Fig. 6G, H). Both residues of the ERα were phosphorylated in the *Pten* CKO
209 compared with control animals (Fig. 6I). On the other hand, expression of growth factor
210 mRNAs that are considered to be targets of ERα [8] was not significantly changed
211 between controls and *Pten* CKO mice (Fig. 6J). Although, phosphorylation of ERα has
212 been implicated in estrogen-independent cell proliferation and differentiation [8, 9], these
213 results suggest that phenotypes induced by *Pten* loss-of-function are independent of
214 ERα signaling.
215
216 *Estrogen-dependent localization of phosphorylated Akt in mouse vagina*
217 Lastly, we examined potential differences in Pten function among several
218 stratified and squamous epithelia in mice. Numerous studies have shown that Pten
219 exerts its tumor suppressive function through inhibition of Akt activation; therefore, it is
220 generally believed that a major Pten function is regulation of cell proliferation in such
221 organs. We found that Pten is mainly expressed in the basal cells in stratified and
222 squamous epithelia, such as epidermis of the skin, tongue, esophagus and forestomach,
223 although Pten expression levels vary among these tissues (Fig. 7A-D). Consequently,